RESERVE THIS SPACE

Investigating the Energetics of Bioadhesion on Micro-engineered Siloxane Elastomers

Characterizing the Topography, Mechanical Properties and Surface Energy and its Effect on Cell Contact Guidance

Adam W. Feinberg[1,2], Amy L. Gibson[2], Wade R. Wilkerson[1,2], Charles A. Seegert[1,2], Leslie H. Wilson[2], Lee C. Zhao[1,2], Ronald H. Baney[2], James A. Callow[3], Maureen E. Callow[3], Anthony B. Brennan[1,2]

[1]Biomedical Engineering Program, University of Florida, Gainesville, FL 32611
[2]Department of Materials Science & Engineering, University of Florida, Gainesville, FL 32611
[3]University of Birmingham, School of Biosciences, Birmingham, B15 2TT, UK

The energetics of a polydimethylsiloxane (PDMS) elastomer biointerface were micro-engineered through topographical and chemical modification to elicit controlled cellular responses. The PDMS elastomer surfaces were engineered with micrometer scale pillars and ridges on the surface and variable mechanical properties intended to effect directed cell behavior. The topographical features were created by casting the elastomer against epoxy replicas of micropatterned silicon wafers. Using UV photolithography and a reactive ion etching process, highly controlled and repeatable surface microtextures were produced on these wafers. AFM, SEM and white light interference profilometry (WLIP) confirmed the

RESERVE THIS SPACE

high fidelity of the pattern transfer process from wafer to elastomer. Ridges and pillars 5 μm wide and 1.5 μm or 5 μm tall separated by valleys at 5 μm, 10 μm, or 20 μm widths were examined. Mechanical properties were modulated by addition of linear and branched nonfunctional trimethylsiloxy terminated silicone oils. The modulus of the siloxane elastomer decreased from 1.43 MPa for the unmodified formulation to as low as 0.81 MPa with additives. The oils had no significant effect on the surface energy of the siloxane elastomer as measured by goniometry. Two main biological systems were studied: spores of the green alga *Enteromorpha* and porcine vascular endothelial cells (PVECs). The density of *Enteromorpha* spores that settled increased as the valley width decreased. The surface properties of the elastomer were altered by Argon plasma, radio frequency glow discharge (RFGD) treatment, to increase the hydrophilicity for PVEC culture. The endothelial cells formed a confluent layer on the RFGD treated smooth siloxane surface that was interrupted when micro-topography was introduced.

Introduction

Understanding the role of surface topography and chemical functionality on adhesion and proliferation of cells to biomaterials is critical in developing and improving biointerfaces. Many of the current limitations of existing devices and problems associated with developing technologies is the inability to start, stop and otherwise control biological growth, i.e., biofouling. Beginning with the deposition of proteins and complex carbohydrates on a surface, the resulting biological cascade can induce unwanted and irreversible effects[1]. Therefore, it is crucial to develop engineered biosurfaces that can elicit a desired cellular response.

While many researchers have evaluated cellular response to topographically and chemically modified polymer surfaces and have observed qualitative effects, few have correlated these results with an in depth characterization of the bulk and surface properties of the material[2-6]. In this paper, an analysis of the interfacial energies of the system is presented through characterization of the mechanical and morphological properties and surface energy of the biomaterial.

The goal is to characterize the bioadhesive properties of the biologically active polymer surface.

Siloxane elastomers were chosen for the model polymer system because of the broad applications ranging from anti-fouling marine coatings to acute and chronic use medical devices. In particular, silicone elastomers represent a class of materials with a well understood chemistry, ease of manufacturability and extensive data on performance in biological systems. The engineered siloxane elastomer surfaces, in this study, have a combination of spatially controlled topographical and chemical modification. Features on the scale of 5 μm to 20 μm have been shown to influence cell function in the literature and these results have been replicated with patterns of ridges and pillars in these experiments[3-5,7-9]. Nonfunctional silicone oils were added to the bulk siloxane elastomer to determine the effects on modulus and surface energy. Due to a lower surface energy, silicone oils segregate to the surface, hence changing bulk properties on a macroscopic scale and imparting liquid like properties to the surface. We theorize that both topographical and chemical features define the surface energy, which in combination with elastic modulus, will dictate biological activity.

In order to understand the biological response to the surface, two types of cell were allowed to attach on the microengineered siloxane elastomers. Settlement (attachment) of motile spores of the marine fouling alga *Enteromorpha* was studied to evaluate the anti-fouling and foul release performance of the surface for marine applications. Porcine vascular endothelial cells (PVECs) were cultured on the surfaces as a model system to determine the bioactivity for potential medical applications such as vascular grafts and orthopedic implant coatings. The grooves formed on these substrates have shown significant control over growth directions of cells. This phenomenon, commonly referred to as "contact guidance," typically demonstrates cellular alignment along the grooves depending on the dimensions of the features. Current literature focuses on the mechanisms behind the alignment of these cells to the surface topography. An area of investigation is whether the actual geometries of the features were the defining factor or the change in surface free energy due to edges and disruptions in the planar surface[10]. It has been demonstrated that parameters such as surface free energy and hydrophilicity influence cell growth, but not necessarily the shape or orientation of cells[3]. With the addition of silicone oils on the molecular level and surface texture on the microscopic level, a hierarchical model was developed and examined to determine its effects on biological adhesion.

Experimental

Substrate Production

The micropatterned surface was initially etched into a silicon wafer using the Bosch process. The patterns chosen were 5 µm ridges separated by 5 µm, 10 µm and 20 µm valleys and 5 µm high cubes separated by 5 µm, 10 µm and 20 µm as seen in figure 1. These features were on the same size scale as cells and have been shown in the literature, and our own observations, to influence cell growth. Standard photolithographic microprocessing was used to fabricate the patterns, briefly: wafers were coated with photoresist (Clariant AZ1529 positive photoresist) and then exposed to UV light through a photomask. The photoresist was developed and the wafers were etched to a depth of 5 µm (Unaxis, Tampa, FL) or etched to a depth of 1.5 µm (University of Florida). Wafers were etched to a depth of 5 µm at Unaxis using the Bosch process to obtain nearly vertical sidewalls. This was in contrast to the 1.5 µm deep features produced at the University of Florida (UF) where a standard reactive ion etcher (RIE) produced sloping features due to lower anisotropy in the vertical direction. Molds were made of the etched wafers using the PDMS elastomer and then used to make nearly identical copies of the silicon wafer using a low shrinkage epoxy (Epon 828 with Jeffamine D230). These epoxy copies then became the masters for mass replication with siloxane elastomer and the original silicon wafer was stored to maintain the original pattern.

Silastic T-2 (Dow Corning) was chosen for its excellent dimensional stability, self-degassing properties and optical transparency (for laser confocal and light microscopy). It was also chosen because there were minimal unknown or non-disclosed additives, allowing for comprehensive control of additives and chemical modifications. The platinum catalyzed hydrosilylation cured siloxane elastomer was mixed in a 10:1 wt/wt base resin to curing agent ratio as specified by the manufacturer. It was then degassed under vacuum for 20 minutes and cast on the epoxy copies. Samples were then cured for 24 hours at room temperature before removing from the mold.

Silicone oils of linear structure were added to the Silastic T-2 during mixing and then cured to vary bioadhesive properties. Due to the nonfunctional trimethylsiloxy terminated polydimethylsiloxane oils used, no chemical incorporation of the oils into the vinyl functionalized elastomer occurred. Energetics dictate that the oils wet the siloxane elastomer surface, thus a controlled release of the oils to the surface occurs. The linear silicone oils chosen were 50 cSt, 500 cSt and 5000 cSt viscosities, which correlates with molar mass of 3.8, 17.3 and 49.4 kg/mol respectively, as reported by the

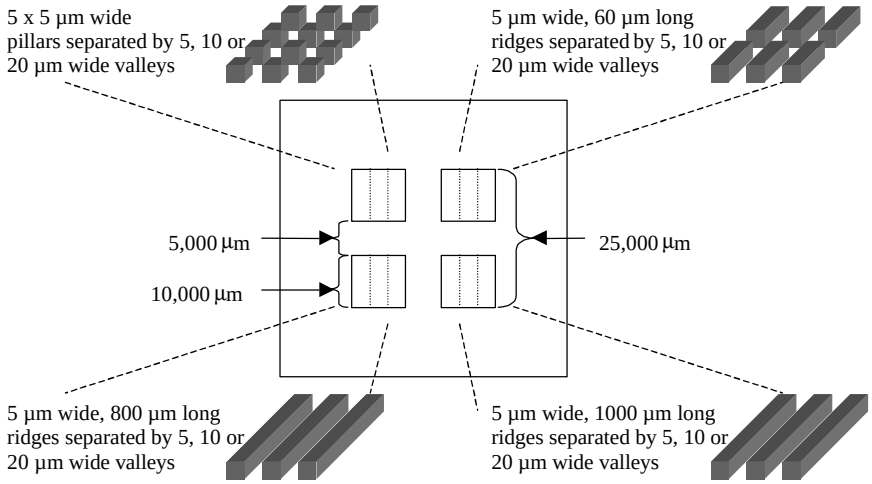

Figure 1: Layout of the micro-patterned substrate etched to 1.5 mm or 5 mm depth. There were four 1 cm^2 main areas each with the feature type indicated in the diagram. Each main area was subdivided into three smaller 1/3 cm^2 areas with either 5, 10 or 20 mm spacing between features.

manufacturer (Gelest Inc.). In addition, low molar mass, non-functional, branched oils tetrakis(trimethylsiloxy)silane and tris(trimethylsiloxy)silane of 385 g/mol and 297 g/mol respectively (Gelest Inc.) were used as additives. The oils were mixed independently into the Silastic T-2 at 5%, 10% or 20% by weight prior to cure.

Morphological Analysis

Verifying the uniformity and consistency of dimensions in the micropatterning process was necessary to ensure the engineered patterns were properly transferred to the elastomer surface. This was accomplished with a combination of scanning electron microscopy (SEM), atomic force microscopy (AFM) and white light interference profilometery (WLIP). The SEM (Jeol 6400) allowed high magnification of the surface in order to identify defects and irregularities. Samples were coated with Au/Pd and examined at magnifications from 100x to 5,000x. AFM (Digital Instruments Nanoscope IIIa controller operating a Dimension 3100 scanner) operated in tapping mode in air provided the 3-dimensional shape to be observed although artifacts were potentially introduced due to the high aspect ratio of some features. The WLIP (Wyko NT 1000, Veeco Metrology) was operated in vertical scanning-interferometry (VSI)

mode and used white light interference fringes to reconstruct the surface topography in a non-contacting and nondestructive manner. Images were processed using the Vision32 software package (Veeco Metrology) to examine the 3-dimensional topography and 2-dimensional height profiles of the surface.

Mechanical Properties

Tensile specimens were cut from cured 1 mm thick silicone films using an ASTM D1822-68 type L dog bone die. Tensile measurements were made according to ASTM D412-97 on an Instron model 1122 equipped with TestWorks 3.07 software for analysis. Strain measurements were based on crosshead displacement of 2 inches per minute. It is acknowledged that some slippage at the grips did occur, future studies will address this error through use of a laser extensometer. The various surface topographies were not evaluated with this method because the small feature size was insignificant to the bulk properties.

Surface Energy

Contact angles were obtained with a goniometer using the sessile bubble technique for all siloxane elastomer formulations within seconds of placement. Zisman plots were constructed from the contact angles of 2 μL droplets each of HPLC grade water, methylene iodide, 1-propanol, N,N-dimethylformamide and acetonitrile to extrapolate substrate surface energy (n=20 per liquid, per elastomer type)[11,12]. The effect of the oil additives and micro-topography on surface energy were evaluated by the Wilhelmy plate technique using a Cahn DCA. PDMS elastomer strips were used with dimensions approximately 10 mm wide, 30 mm long and 3 mm thick for the smooth, non-textured films, but varied for the textured surfaces since they were cast off an epoxy copy with no back plate. The micro-texture was only on one side and both textured and smooth samples were dipped into HPLC grade water (Fisher Scientific) at a dipping rate of 100 μm/sec.

***Enteromorpha* Studies**

Glass cover slips coated with microtextured siloxane elastomer were evaluated at the University of Birmingham, UK, for attachment studies of the green alga *Enteromorpha* spore. The samples were soaked in sterile seawater overnight and then incubated with *Enteromorpha* spores at ~2 x 10^6 spores/cc

density for 1 hour[13]. The surfaces were then rinsed, fixed, and examined using a Zeiss imaging system attached to a fluorescent microscope to determine the density of settled (attached) spores on each surface.

Endothelial Cell Culture

The elastomer samples were first treated with argon RFGD plasma to increase hydrophilicity and then sterilized with ethylene oxide. The silica-like surface layer created by the plasma treatment is hydrophilic after exposure and then slowly reverts back to a hydrophobic state[14]. Gedde et al have indicated that hydrophobic recovery occurs by oligomer PDMS from the bulk recoating the surface by diffusion through the silica-like layer or through cracks in the silica-like layer caused by mechanical stress. An exposure time of 5 minutes at 50 mW and 4 cm distance from the RF coil prevented measureable hydrophobic recovery in the 5 days between plasma treatment and cell seeding. Individual feature types were separated and cultured in standard polystyrene culture 24 well plates with vascular porcine endothelial cells. For culture, RPMI 1640 medium (Life Technologies, Grand Island, NY) containing antibiotics (100 units/ml of penicillin, 100 µg/ml of streptomycin, 20 µg/ml of gentamicin, and 2 µg/ml of Fungizone) was used. There was no serum added during the culture process. Samples were incubated in 5% CO_2 atmosphere for 3 days to allow cells to reach confluence. Samples were removed, fixed in a 10% formalin solution, stained with crystal violet and then examined under light microscopy.

Results and Discussion

Morphology

SEM, AFM and WLIP images indicate the high fidelity reproduction of the silicon wafer micropattern in the PDMS elastomer. Typical SEM and WLIP images of the silicon wafer, epoxy copies and siloxane elastomer replicates reveal a surface with varying degrees of visible defects but acceptable overall fidelity. There was no observable loss in any of the micrometer scale dimensions and this was consistent for both ridge and pillar type features. As mentioned in the methods, due to differences in the type of RIE used, the 1.5 µm high features have a sloping sidewall indicative of the lower anisotropic etching process available at UF. An important observation, seen in Figure 2 a-c, was that the pillars did not have a cube-like shape but rather appear cylindrical. This

phenomenon was partly a result of the exposure and development of the photoresist prior to etching. Light scattering led to features that were octagonal instead of square. These areas of the mask were further rounded with repeated levels of polymer replication so that by the end of the process they had attained this nearly cylindrical shape. This same defect also occurs at the ends of the ridges. Occasional nanometer scale defects were seen in the SEM images in figure 2b and 2e due to errors in the replication process. These small defects were unavoidable and have been ignored in terms of evaluating the effect of micrometer scale topographical features. The AFM images in figures 2a and 2d were from a 1.5 μm high pillar and 5 μm high ridges respectively and the sloping side wall was believed to be an imaging artifact due to a combination of feature aspect ratio and TappingMode tip geometry. While limited in the ability to image high aspect ratio features, the AFM indicated extremely smooth planar areas on top of the ridges and pillars and the bottom of the valleys. The WLIP images corroborate the SEM and AFM results and due to the exaggerated z axis scale make the finite radius of curvature of the feature edges visible. The nanometer scale radius of curvature was approximately three orders of

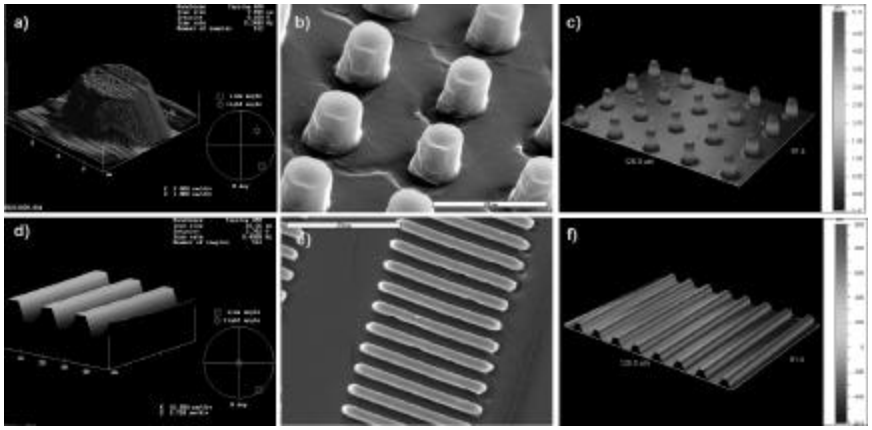

Figure 2: Atomic force micrographs (a and d), scanning electron micrographs (b and e) and white light interference profilometry (c and f) of the microtextured siloxane elastomer surface. The pillars and ridges were easily seen. a) Single 5 mm wide pillar, b) 5 mm high pillars separated by 5 mm valleys, c) 5 mm high pillars separated by 10 mm valleys (Si wafer), d) 5 mm high, 5 mm deep and 800 mm long ridges separated by 10 mm valleys, e) 5 mm high, 5 mm deep and 60 mm long ridges separated by 5 mm valleys, f) 1.5 mm high, 1000 mm long ridges separated by 10 mm valleys (Si wafer).

magnitude smaller than the cell and therefore has not been evaluated in the scope of this paper.

The oils added to the Silastic T-2 can have an impact on the fidelity of the pattern reproduction. This has been examined thoroughly for the 1.5 μm features for the various oil types. The samples with 5000 cSt linear oils added to the Silastic T-2 had a visible oil layer on the surface. The patterns would disappear optically to both the naked eye and WLIP after 24-48 hours indicating that oils were segregating to the surface and filling in the pattern. This behavior was not noticed at the lower oil viscosities. Figure 3 shows a typical profile WLIP image of the 5 μm ridges separated by 5 μm valleys of the 5000 cSt, 20 wt% oil modified elastomer that was achieved by removing the surface oils by wiping with toluene just prior to imaging. The feature height and valley depth should be constant compared to other sample types, but was variable with a measured distance of over 2 μm for the amplitude at some points. Since the epoxy mold was verified to have a ~1.5 micrometer feature height, this change in height of the elastomer was due to surface distortions and possible material loss due to the removal of the 5000 cSt PDMS oils. From these data it was concluded that oil at the surface does change the topography with the effect dependent on oil viscosity and a time dependence on quantity. In terms of the surface seen by microorganisms, the question is whether a particular cell type, in a given biological environment, can displace the oils and contact the underlying solid surface.

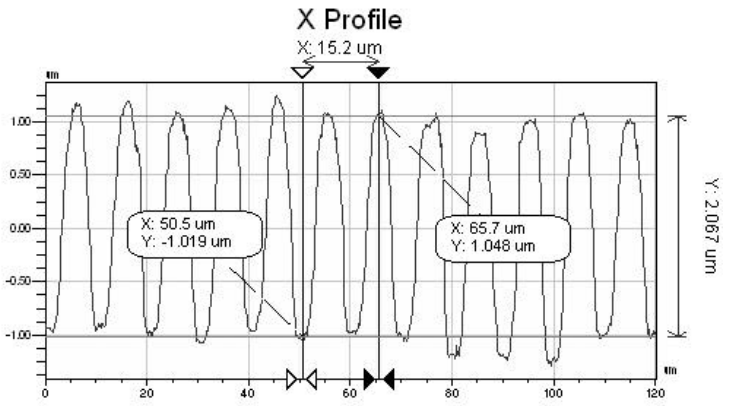

Figure 3: 5000 cSt, 20 wt% oil modified elastomer wiped with toluene immediately before imaging. A 2-dimenional profile WLIP image sliced perpendicular to the long axis of the 5 mm ridges separated by 5 mm valleys. The variation in valley and peak heights can be clearly seen as well as the variable amplitude ranging from 1.7 to 2.5 mm.

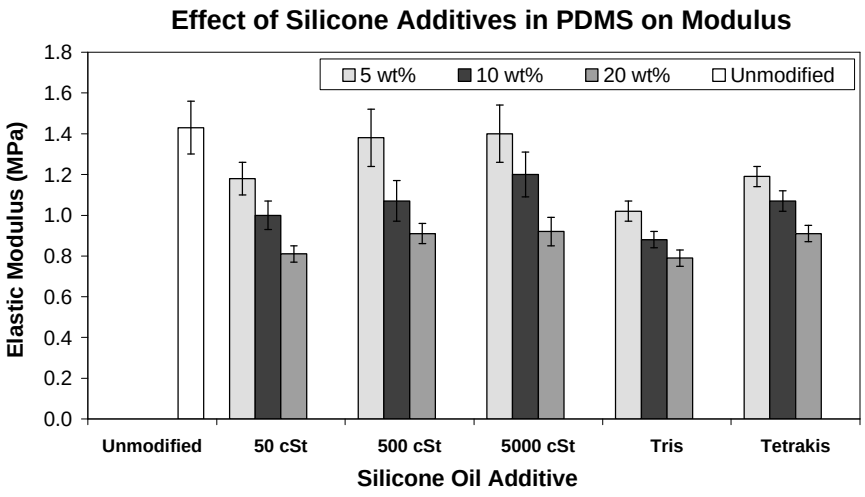

Figure 4: Graph of Young's Modulus obtained from tensile testing for siloxane elastomer modified with non-functional trimethylsiloxy terminated siloxane oils

Mechanical Properties

Instron tensile testing of various nonfunctional silicone oil incorporations yielded less than an order of magnitude change in elastic modulus and was highly dependent on concentration, as shown in Figure 4. Future studies will incorporate functionalized silicone oils that vary the crosslink density thus significantly changing the elastic modulus. Modulus has been shown to be a significant factor in controlling bioadhesion. While traditional theories related the relative adhesion of a surface primarily to surface energetics, it is now recognized that a factor of (surface energy *Elastic modulus)$^{1/2}$ is a better representation[15,16]. This indicates why silicones are found to have lower adhesive values than lower energy surfaces such as higher modulus fluoropolymers.

Surface Energy

Surface energy was changed as a function of the chemical and topographical features of the surface[17,18]. The effect of the oil additives were evaluated using goniometry and DCA. Results for nonfunctional oil additives as well as the unmodified Silastic T-2 elastomer indicated no significant change in surface

energy for any formulation as seen in Table 1. The lower surface tension of the liquid PDMS as compared to the surface energy of the bulk elastomer caused oils to segregate to the surface. Since surface energy analysis was only sensitive for one molecular monolayer, the methyl side groups of the PDMS oils presents a surface that was indistinguishable from the cured elastomer formulations[12,19]. The surface energies were calculated from the contact angles using a modified Zisman plot of Cos θ vs. $1/(\gamma^{1/2})$, applicable to low surface energy materials like PDMS[20]. DCA was used to evaluate the affect oil additives had on the hysteresis of the advancing and receding contact angles as seen in Table 2. The large hysteresis for the first four samples was thought to be due to the rearrangement of the polymer backbones to express more hydrophilic moieties for the receding contact angle. Of note is the significantly smaller hysteresis for the 20% 5000 cSt sample where the visible oil layer seems to have interfered with the surface rearrangement. The effect of micrometer scale topography was evaluated using DCA. Direct measurement of the contact angle was not possible due to software limitations, however, a change in slope of the force verse position curves was observed between the smooth and textured regions. This change in slope, and hence contact angle, indicates that micropatterning causes a measureable difference between the surface energy of different topographical domains.

Table 1: Contact angles and calculated surface energy of PDMS elastomer modified with non-functional silicone oils

Samples	*Water*	*MeI*	*DMF*	*ACN*	*1-Prop*	g_c *(mN/m)*
Unmodified	109.1 ± 3.5	67.2 ± 3.8	54.5 ± 2.1	46.7 ± 3.5	31.5 ± 2.1	23.0 ± 0.4
5% 50 cSt	110.3 ± 2.6	65.5 ± 1.4	55.7 ± 2.2	44.2 ± 2.8	30.6 ± 1.4	23.3 ± 0.3
20% 50 cSt	109.2 ± 1.4	64.0 ± 2.3	54.3 ± 2.2	45.8 ± 2.8	24.5 ± 1.4	23.7 ± 0.4
5% 5000 cSt	107.7 ± 2.0	64.6 ± 1.9	54.7 ± 1.3	47.8 ± 1.9	26.1 ± 1.5	23.3 ± 0.2
20% 5000 cSt	103.4 ± 2.4	64.4 ± 1.9	51.9 ± 2.3	48.1 ± 1.8	26.0 ± 1.9	23.1 ± 0.3
20% Tris	106.4 ± 2.3	64.3 ± 2.3	55.5 ± 1.8	46.2 ± 1.9	28.8 ± 1.2	23.1 ± 0.2

Table 2: DCA Data for PDMS elastomer modified with non-functional oils

Viscosity	*Wt. %*	q_{adv}	q_{rec}	*Dq*
No Oil	N/A	115.1 ± 3.8	68.7 ± 2.2	46.4 ± 1.7
50 cSt	5%	113.9 ± 1.8	77.5 ± 1.8	36.4 ± 0.3
50 cSt	20%	100.5 ± 1.3	65.1 ± 2.1	35.4 ± 1.6
5000 cSt	5%	106.1 ± 0.7	71.6 ± 2.2	34.5 ± 2.1
5000 cSt	20%	100.9 ± 1.1	91.8 ± 2.4	9.1 ± 1.3

Bioadhesion Studies on *Enteromorpha* spores and Porcine Vascular Endothelial Cells (PVECs)

Preliminary *in vitro* cell culture studies demonstrate that the type of contact guidance and bioadhesion to the surface was dependent on the cell type. Evaluating the changes in surface topography using the unmodified PDMS elastomer, the textured surfaces showed a substantial increase in spore accumulation compared to non-textured surfaces as seen in Figure 5. The flat elastomer surface provided the least favorable substrate in terms of spore adhesion, and the 5 µm widths between features had the greatest spore accumulation. This increase in spore density on smaller widths also corresponds to the highest density of microfeatures, which may also be related to the length of the feature. The spores appeared to attach inside the grooves in the angle between the valley floor and the side wall.

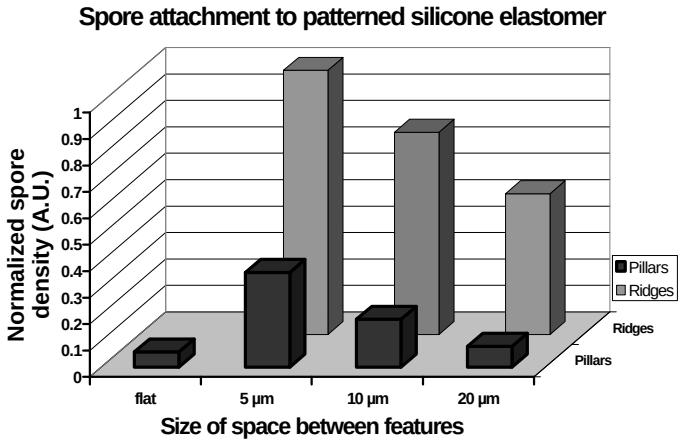

Figure 5: Spore attachment to patterned silicone elastomer. Features were 5 µm high.

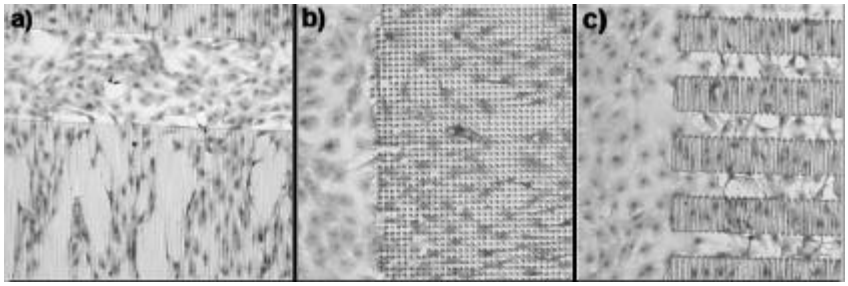

Figure 6: Optical microscopy of stained PVECs on a textured RFGD treated siloxane elastomer substrate. a) smooth and 5mm high, 1000 mm long textured ridges (10X), b) 5 mm high textured pillars (10X), c) smooth and 5mm high, 60 mm long textured ridges (10X).

Preliminary endothelial cell (EC) studies show a decrease in confluence on textured surfaces. Figure 6 are light microscope images of stained EC's on textured siloxane substrate. The cells form a confluent layer in the smooth region, but were less dense on the ridge and pillar areas. This disruption of the normally confluent endothelial cell mono-layer suggests that these types of patterns might be appropriate for medical applications where cell adhesion is undesirable, such as surgical adhesions.

Conclusions

The ability to characterize the surface and bulk properties of biomaterials is essential in understanding how they influence cellular adhesion and growth. The results of this paper demonstrate the ability to both evaluate and control the topographical and chemical features engineered into siloxane elastomers. The AFM, SEM and WLIP images are evidence that the replication of the micropatterned silicon wafer was high fidelity limiting the possible topographies to the capabilities of the micromachining process itself. The mechanical analysis indicates that surfaces can be engineered with varying moduli to moderate interactions with specific cell types. Combining these findings with qualitative evaluations of *in vitro* cell culture and *in vivo* device implants will allow modeling of the cellular response to morphological, mechanical and surface energy properties. The goal is to develop reliable models for different cell types to engineer specific surfaces for each unique biological application.

Two main biological systems were studied: spores of the marine green alga *Enteromorpha* and porcine vascular endothelial cells. Spores settled preferentially onto the microtextured surfaces and the density of attached spores increased as the space between features decreased. The endothelial cells appear

to prefer the smooth siloxane surface and the confluence of cell coverage was decreased when micro-topography was introduced. From these results, it is clear that the cell type has a significant impact on the response to micro-engineered surfaces. The complexity of biological systems requires a better fundamental understanding of the substrate/cell interface in order to engineer biomaterials for specific applications.

Acknowledgements

The authors acknowledge the financial support of the Office of Naval Research (US Navy N0014-99-1-0795) to fund this research. The 5 μm deep micropatterned silicon wafers were reactive ion etched by Abdul Latif at Unaxis (Tampa, FL). We thank the research group of Dr. Edward R. Block for supplying endothelial cells, and C. Keith Ozaki, M.D. and Zaher Abouhamze, B.S. for technical assistance and advice.

References

1. *Biomaterials Science: An Introduction to Materials in Medicine*; Ratner, B.D.; Hoffman, A.S.; Schoen, F.J.; Lemons, J.E., Eds.; Academic Press: San Diego, CA, 1996.
2. Curtis, A., Wilkinson, C. *Biomaterials* **1997**, *18*, 1573-1583.
3. den Braber, E.T., de Ruijter. *Journal of Biomedical Materials Research* **1995**, *29*, 511-518.
4. Flemming R.G., Murphy C.J., Abrams G.A., Goodman S.L., Nealey P.F. *Biomaterials* **1999**, *20(6)*, 573-588.
5. Bahatia, S.N.; Chen, C.S. *Biomedical Microdevices* **1999**, *2:2*, 131-144.
6. Singhvi, R., Kumar, A., Lopez, G.P., Stephanopoulos, G.N., Wang, D.I.C., Whitesides, G.M., Ingber, D.E., *SCIENCE* **1994,** *264*, 696-698.
7. Tan, J., Shen, H., Carter, K.L., Saltzman, W.M. *J. Biomed. Mater. Res.* **2000,** *51*, 694-702.
8. Folch, A., Byong-Ho, J., Hurtado, O., Beebe, D.J., Toner, M., *J. Biomed. Mater. Res.* **2000**, *52*, 346–353.
9. *Cell Adhesion: Characterization of Adhesive Forces and Effect of Topography*, Zhao, L.C., Masters of Science Thesis, University of Florida, Gainesville, FL, 2000.
10. von Recum, A.F. and T.G. Van Kooten. *J. Biomater. Sci. Polymer Edn.* **1995**, *7(2)*, 181-198.
11. Johnson, R.E. and Dettre R.H. *Surface and Colloid Science* **1969,** *2,* 85-153.

12. Good, R.J. *J.Adhesion Sci. Technol.* **1992,** *6(12)*, 1269-1302.
13. Callow, M.E., Callow, J.A., Pickett-Heaps, J.D., Wetherbee, R. *Journal of Phycology* **1997**, *33*, 938-947.
14. Hillborg, H., Sandelin, M., Gedde, U.W. *Polymer* **2001,** *42(17)*, 7349-7362.
15. Kohl, J.G. and Singer I.L. *Progress in Organic Coatings* **1999**, *36*, 15-20.
16. Brady, R.F. and Singer, I.L. *Biofouling* **2000**, *15(1-3)*, 73-81.
17. Oner, D. and McCarthy, T.J. *Langmuir* **2000**, *16*, 7777-7782.
18. Schmidt, J.A. and von Recum, A.F. *Biomaterials* **1992**, *13(10)*, 675-681.
19. Shafrin, E.G. and Zisman W.A. *Langmuir* **1960**, *64*, 519-524.
20. Good, R.J., *J. Ahesion Sci. Technol.*, **1992,** *6(2)*, 1269-1302.